

Preparation and characterization of a dual acidic Ionic Liquid functionalized Graphene Oxide nanosheets as a Heterogeneous Catalyst for the Synthesis of pyrimido[4,5-b] quinolines in water

Mohanad Yakhdan Saleh^{a*}, Ghufran Th. Sadeek^a, Shakir Mahmood Saied^b

a) Department of Chemistry, College of Education for pure Science, Mosul University, Ministry of High Education and Scientific Research, Mosul, Iraq

b) Department of Medical Laboratory Techniques, Al-Noor University College, Iraq

Received 8 October 2023; received in revised form 22 November 2023; accepted 26 November 2023 (DOI: 10.30495/IJC.2023.1998276.2052)

ABSTRACT

Pyrimido[4,5-b]quinolones play a significant role in medicinal chemistry owing to their various biological properties, including antihistaminic, antimalarial, antifungal, anticancer, antioxidant, antiviral, anti-microbial, and anti-inflammatory activities. A dual acidic ionic liquid anchored on graphene oxide nanosheets (GO-Si-Pr-Lysin-SO₃H) was provided and characterized using transmission electron microscopy (TEM), scanning electron microscopy (SEM), X-ray diffraction (XRD), thermogravimetric analysis (TGA), and Fourier transform infrared spectroscopy (FT-IR). The six-step process was utilized to create this catalyst, beginning with graphite powder. This catalyst was capable to develop the one-pot and three components (6-amino-1,3-dimethyluracil, dimedone, and different aromatic aldehydes) synthesis of pyrimido[4,5-b]quinolone derivatives at moderate temperature in water as a green medium (12 derivatives). The results obtained indicated that this method could be an effective approach for synthesizing pyrimido[4,5-b]quinolones with high yields ranging from 86% to 98% in a short reaction time of 15 to 40 minutes. In addition, the pointed catalyst shows reusability and recoverability without remarkable loss of catalytic activity.

Keywords: Green catalyst; ionic liquid; graphene oxide; pyrimido[4,5-b]quinolones; reusability

1. Introduction

A quinolone antibiotic compound is a member of a vast group related to the substance 4-quinolone [1]. In the Human body, antibiotics kill or inhibit the growth of bacteria [2-4]. The fluoroquinolones are nearly compounds to the quinolones antibiotic, which involve a fluorine atom in their chemical structure and these compounds are effective against both Gram-negative and Gram-positive bacteria. The ciprofloxacin, levofloxacin, norfloxacin, besifloxacin, and moxifloxacin are some of the quinolones containing fluorine atoms. The chemical structure of some of the drugs based on the quinolone derivatives is shown in **Fig. 1**. The mechanism of drugs based on quinolone was occurred during interfering DNA replication using

preventing bacterial DNA from unwinding and duplicating. The active structure or basic pharmacophore of the quinolone unit is based upon the ring system that highlighted is as blue color in **Fig. 1**.

According to the importance of quinolone drug substances, an important category of hetero-cycles involving nitrogen is pyrimido[4,5-b]quinolone derivatives, which could be produced using the one-pot, and multicomponent reaction of aldehydes, 6-amino-1,3-dimethyluracil, and dimedone. Up to now, some of the catalysts have been used for the preparation of pyrimido[4,5-b]quinolone derivatives [5-24] (**Scheme 1**). The previous reported catalysts have several disadvantages, including the use of metal catalysts, the use of hazardous organic solvents, non-recoverable catalysts, excess amount of catalyst, expensive reagents, extended time of the reactions, and so on. Therefore, the

*Corresponding author:

E-mail address: mohanadalallaf@uomosul.edu.iq (M. Y. Saleh)

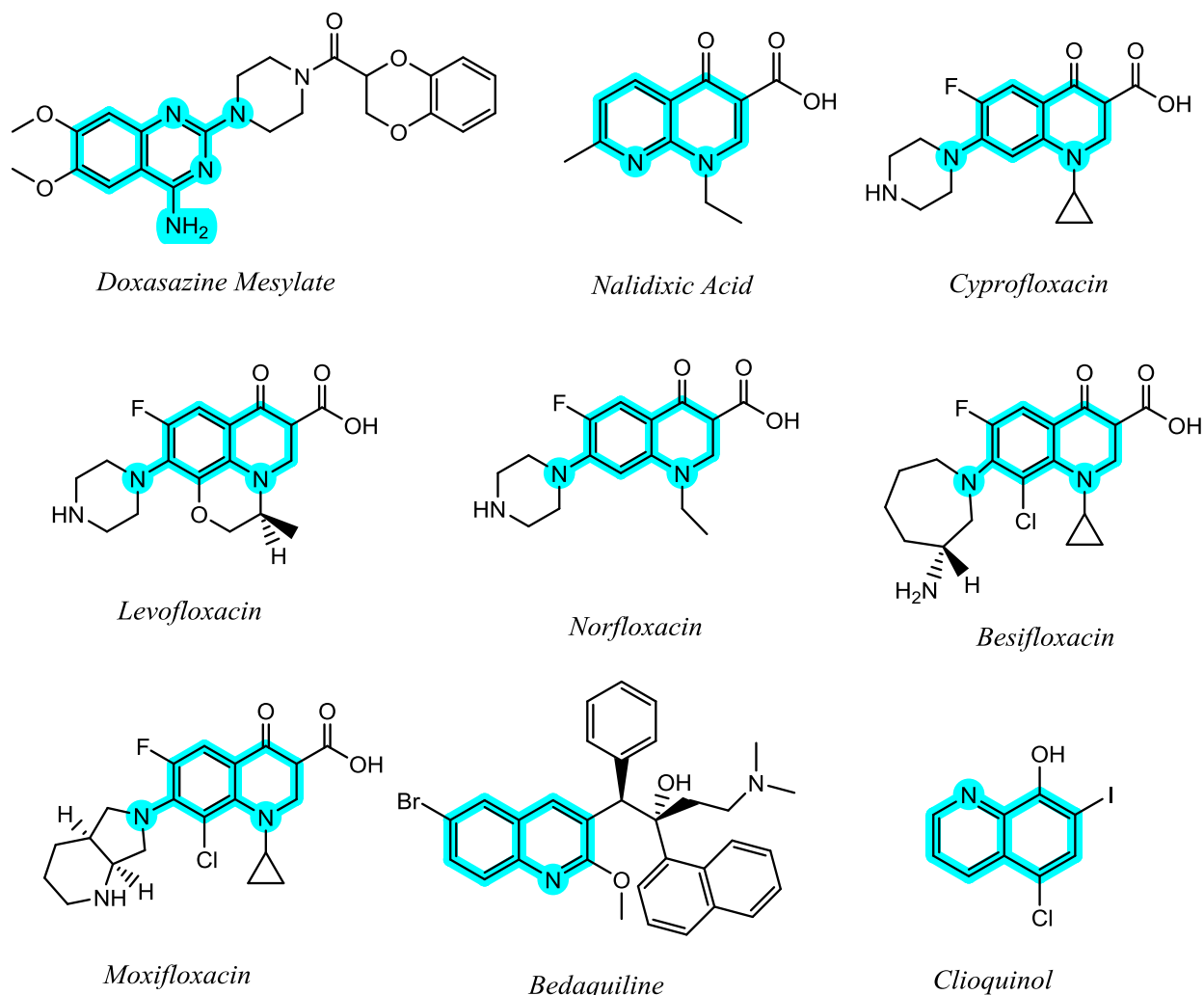
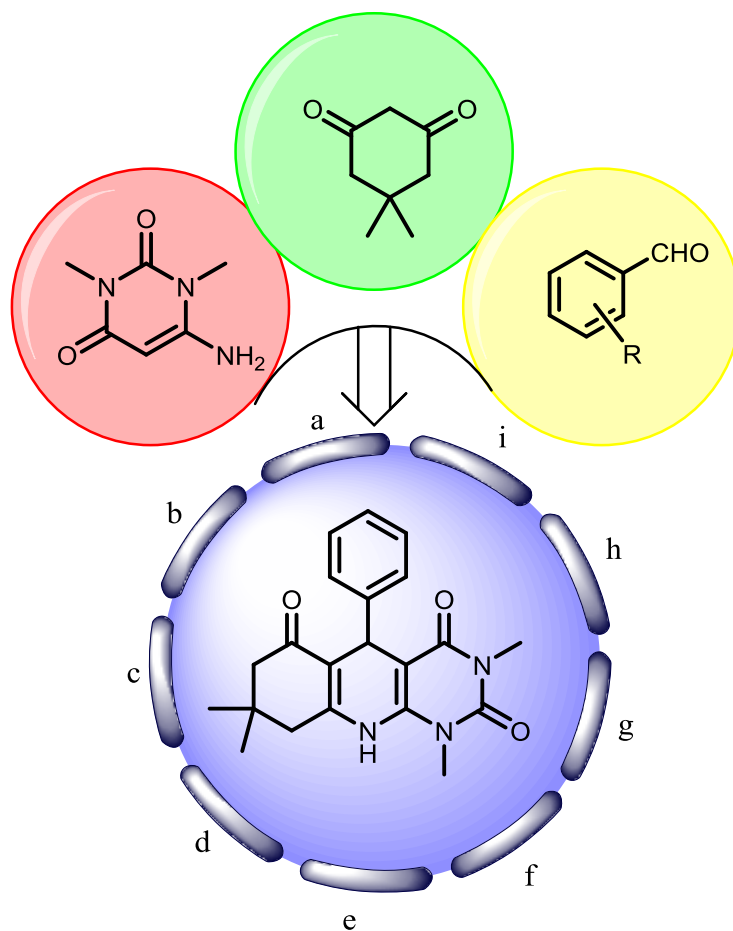


Fig. 1. The structure of some of the medicinal drugs based on the quinolone ring system.

design and preparation of superior and robust heterogeneous catalyst is still in demand for providing of pyrimido[4,5-b]quinolones using a greener and high-yielding method.

In 2008, Li and co-workers reviewed the materials based on graphene as a major scientific research topic [32]. The large specific surface area, approximately $2600 \text{ m}^2 \cdot \text{g}^{-1}$, is the best factor for the application of graphene-based materials as support for heterogeneous catalysts [33, 34]. Up to now, a lot of organic transformations have been performed using functionalized graphene and graphene oxide as support or heterogeneous catalyst [35-62]. These catalytic systems show high efficiency, high turnover number (TON), high stability towards chemical and thermal conditions, and worthwhile reusability. In addition, Ionic liquids (ILs) hold immense importance in various scientific and industrial

domains [63, 64]. Organic synthesis has significantly benefited from the use of acidic ionic liquid catalysts [65-67]. Grafting solid supports (nano or bulk materials) onto ionic liquids enables the heterogenization process, resulting in catalysts that possess the combined benefits of both ILs and heterogeneous catalysts. It is comparatively simpler to handle, isolate, recycle, and reuse heterogeneous catalysts in comparison to homogeneous catalysts. Based on the reported data for graphene support, it is the best choice for election as a superior support for the target method. Furthermore, as part of our ongoing research [68-70], we endeavored to employ green functionalized groups for the purpose of anchoring onto the surface of graphene nanosheets. In this regard, the special ionic liquid was modified and anchored on the surface of graphene oxide nanosheets.



Scheme 1. Some of the synthetic approaches for the providing of pyrimido[4,5-b]quinolone a) 1,4-diazabicyclo[2.2.2]octane-1,4-dium HSO₄, solvent: Ethanol: Water, Time: 2.083 h, T: 75 °C, Yield: 95% [7]. b) Cellulose@Fe₃O₄ nanoparticles, solvent: water, Time: 2 h, T: reflux, Yield: 92% [25]. c) DMF, heating, Time: 2h, Yield: 88% [26]. d) *p*-Tol-SO₃H, solvent: water, Time: 2.5 h, T: 90 °C, Yield: 88% [27]. e) 1-n-butyl-3-methylimidazolium bromide, Time: 3h, T: 95 °C Yield: 87% [28]. f) 1,3-disulfonic acid imidazolium hydrogen sulfate, solvent: Ethanol, Time: 0.583 h, T: 70 °C, Yield: 86% [29]. g) Rhodium (III) chloride hydrate, solvent: water, Time: 0.1333 h, T: 40 °C, ultrasound irradiation, Yield: 80% [30]. h) Zirconium hydrogen sulfate, solvent-free, Time: 1h, T: 80 °C, Yield: 96% [31]. i) nano-[Fe₃O₄@-SiO₂@R-NHMe₂][H₂PO₄], solvent-free, Time: 0.1666 h, T: 120 °C, Yield: 94% [12].

2. Experimental

2.1. General remarks

6-Amino-1,3-dimethyluracil (**1**), dimedone (**2**), various aromatic aldehydes (**3**), inorganic reagents, and powder of graphite were procurement from Merck company. The pointed materials and compounds were applied without further purification. The ¹³C and ¹H Nuclear Magnetic Resonance (NMR) spectra were obtained on (DRX Bruker) 500 MHz spectrometer. Chemical shifts (δ) (based on ppm) are released relative to deuterated dimethylsulfoxide (DMSO-d₆) as a solvent: references for DMSO-d₆ were 39.93 ppm (¹³C NMR) and 2.48 ppm (¹H NMR). In ¹H NMR spectra the multiplet, singlet, doublet, triplet, and doublet of doublet were known as

m, s, t, d, and dd, respectively. The elemental analysis (Carbon, Hydrogen, Nitrogen) were recorded from a Carlo-ERBA (EA-1108 Model) instrument. The Perkin-Elmer 781 spectrophotometer was utilized to record FT-IR spectra as KBr pellets within the 400-4000 cm⁻¹ range. The X-ray diffraction (XRD) pattern of the given graphene oxide and catalyst samples was obtained using a Philips device equipped with a Cu anode material. The X-ray beam had a wavelength of 1.54 Å, and the scanning rate was set at 2° per minute within the range of 10° to 80° (2θ). The Mettler-TA4000 instrument's TG-50 Model was utilized to conduct TGA at a heating rate of 10 K min⁻¹ under an inert nitrogen atmosphere. The FESEM S4160 Hitachi device was utilized to investigate the size and shape of the GO-Si-Pr-Lysin-SO₃H morphology. The electron acceleration voltage (V₁₁) of 80 kV was utilized by (EM10C-Zeiss) to

provide the TEM images. The melting points (M. P.) of synthesized compounds had been acquired with a Thermo-scientific micro melting factor tool using open capillary tubes and are uncorrected. The monitoring and development of the organic reactions were performed using TLC on a silica gel plate with type poly Gram SILG/ UV 254.

2.2. Providing of graphene oxide (GO) nanosheets

The optimized Hummer's method prepared the GO nanosheets from graphite powder [71]. Typically, a mixture of 10.0 g of graphite powder and 5.0 g of NaNO_3 is combined with 230 mL of H_2SO_4 (98%) in a 2500 mL flask equipped with a condenser and magnetic stirrer, which is then placed in an ice bath. The solution that was obtained was mixed and slowly incorporated 30.0 g of KMnO_4 . The blend was mixed for a prolonged period of 2 hours. The mixture flask was transferred to a water bath set at 35°C and mixed for a prolonged period of 30 minutes. Subsequently, a gradual addition of 460 mL of deionized water was made to the mixture while maintaining the temperature at around 98°C . The mixture was then blended for an additional 15 minutes. Subsequently, 1400 mL of DI- H_2O and 100 mL of hydrogen peroxide (30%) were consecutively added to the mixture to stop the major and minor reactions. The provided mixture was purified and washed with hydrochloric acid (5 v/v%) then followed by water at various times. The mixture was purified using a vacuum pump over sinter-glass (G4) under reduced pressure. After drying in oven supplied with a vacuum pump for 12 h at 60°C , the graphite oxide was provided. These materials were dispersed in H_2O to build a solution involving 0.5 mg mL^{-1} , and separated sheets utilized ultrasound irradiation (45 watt) for 30 min to provide graphene oxide nanosheets, tracked by centrifugation for 30 min at 3500 rpm to eliminate un-exfoliated graphite oxide.

2.3. Synthesis of the GO-Si-Pr-Cl

The process involved introducing graphene oxide nanosheets into a two-neck flask equipped with a condenser and magnetic stirrer, all under a nitrogen gas environment. A mixture of 2.0 g graphene oxide nanosheets and 10.0 mL 3-chloropropyltrimethoxysilane was then added to 50 mL of dry toluene as the solvent, and the mixture was refluxed for 6 hours. Upon finishing the reaction, the mixture underwent a gradual cooling process until it reached room temperature. Subsequently, it was filtered through sinter glass and then washed using dry toluene. The resulting functionalized graphene oxide with three-

chloropropyltrimethoxysilane (GO-Si-Pr-Cl) was then loaded into a desiccator system under N_2 surroundings.

2.4. Evaluation and determination of Cl on the surface of GO-Si-Pr-Cl

In order to determine of chlorine atoms on the surface of GO-Si-Pr-Cl the Mohr's approach was applied to measure the content of chlorine atoms of 3-chloropropylsilyl groups supported on graphene oxide nanosheets. Initially, 500 mg of GO-Si-Pr-Cl was spread out in H_2O (50 mL), and 50.0 mL of sodium hydrogen carbonate (0.0053 M) was added to the GO-Si-Pr-Cl. Afterwards, the mixture was supplied using ultrasound irradiation for 2.0 min. Later, the mixture was blended for 60 min h at room temperature. Afterward, the materials were filtered over grade 4 of sinter glass and perfectly washed various times with water. Therefore, the solution has NaCl together with the excess amount of NaHCO_3 . At the moment, we might measure the content of chlorine ions in solution by Mohr's approach. The pH of the mixture may be between 6.5 and 10. This approach determines the chloride ion concentration of the obtained solution by titration with AgNO_3 . As the AgNO_3 is unhurriedly added, a precipitate of AgCl (s) forms. The titration is complete when all of the chloride ions have been precipitated. Ag ions are then treated with the CrO_4 ions of the indicator potassium chromate (K_2CrO_4) to form a reddish-brown precipitate of Ag_2CrO_4 . For Mohr's approach, the following items were needed. AgNO_3 (aq): (0.1 M) if possible, 5.0 g of silver nitrate anhydrous for 120 min at 100°C and allow cooling. Accurately weigh about 4250 mg of AgNO_3 (s) and dissolve it in a flask of 25.0 mL of water. Keep the solution in a dark-brown flask. K_2CrO_4 solution as an indicator (about 0.25 M) dissolving 1000 mg of K_2CrO_4 in 20.0 mL of H_2O . According to Mohr's approach, the total of Cl in the GO-Si-Pr-Cl was 1.25 mmol per 1.0 g of GO-Si-Pr-Cl. Therefore, we calculated the amount of Cl-Propyl groups on GO was about 1.25 mmol g^{-1} .

Preparation of the GO-Si-Pr-Lysin- SO_3H nanocatalyst

Using a flask (200 mL) equipped with a magnet and condenser, the nitrogen atmosphere was maintained while lysine monohydrochloride (6.0 mmol), GO-Si-Pr-Cl (1.0 g), and Et_3N (0.4 mL) were added to dry ethanol (50 mL). The mixture was subjected to stirring for 8 hours at 60°C , followed by washing and filtration with NaHCO_3 (aq) at 10%, warm water, and ethanol (4 times of 5 mL each). The GO-Si-Pr-Lysin-Cl was obtained as a dark solid after being dried in a vacuum oven at 60°C overnight. Then, it was added to a flask (200 mL) equipped with a magnet and condenser and purged with nitrogen gas, along with ClSO_3H (2.0 mmol) and absolute ethanol (25 mL), at 40°C for 24 hours while

stirring. Then, 1.0 mL of H₂SO₄ was added and stirred for an additional 3 h. After the suitable time, the solid GO-Si-Pr-Lysin-SO₃H catalyst was washed and filtered with H₂O and C₂H₅OH and dried at 100 °C for 12 h.

General method for the preparation of pyrimido[4,5-b]quinolone using GO-Si-Pr-Lysin-SO₃H

In a round-bottom flask (25.0 mL), a mixture of 6-amino-1,3-dimethyluracil (**1**) (2.0 mmol, 0.31 g), dimedone (**2**) (2.0 mmol, 0.28 g), and different aromatic aldehydes (**3a-3i**) (2.0 mmol), and 30 mg of GO-Si-Pr-Lysin-SO₃H was stirred completely at 50 °C in water as a green and environmental-friendship solvent. After completion of the reaction (monitoring by TLC), the mixture of reaction was slowly cooled to room temperature. Then, 30 mL of EtOAc (Hot) was added, and the catalyst and remained starting materials were filtered. The remaining EtOAc was slowly evaporated to obtain crude products. In order to provide pure products, the crude products were recrystallized from ethanol or water: ethanol (1:1) to obtain highly pure products.

2.5. General method for the reusability of the catalyst

The recovery and reuse of catalysts are crucial from both an economic and industrial perspective in actual practice. Reusability of the GO-Si-Pr-Lysin-SO₃H was investigated in the reaction of 6-amino-1,3-dimethyluracil (**1**), dimedone (**2**), and 2,4-dichlorobenzaldehyde (**3f**), and 30 mg of GO-Si-Pr-Lysin-SO₃H. At the end of each catalytic cycle, 30 mL of ethyl acetate (Hot) was added, and the catalyst and remained starting materials were filtered. For regeneration of the GO-Si-Pr-Lysin-SO₃H, the catalyst was exhaustively washed using C₂H₅OH and water and dried at 80 °C overnight.

Selected spectroscopic information of synthesized compounds

Compound 4a. ¹H NMR (500 MHz, DMSO-d₆): δ (ppm) 9.03 (s, NH, 1H), 7.17-7.24 (m, 4H), 7.02 (1H, t), 4.86 (s, CH, 1H), 3.45 (s, N-CH₃, 3H), 3.09 (s, N-CH₃, 3H), 2.49-2.59 (O=C-CH₂, 2H), 2.20 (d, C=C-CH₂, 1H), 2.01 (d, C=C-CH₂, 1H), 1.01 (s, C-CH₃, 3H), 0.88 (s, C-CH₃, 3H). ¹³C NMR (125 MHz, DMSO-d₆): δ (ppm) 26.80, 27.99, 29.05, 30.55, 32.31, 34.33, 50.41, 90.71, 112.06, 126.25, 127.99, 144.25, 146.32, 150.06, 150.88, 161.23, 194.89.

Compound 4b. ¹H NMR (500 MHz, DMSO-d₆): δ (ppm) 9.04 (s, NH, 1H), 7.25 (5H, aromatic-hydrogen), 4.83 (s, CH, 1H), 3.44 (s, N-CH₃, 3H), 3.06 (s, N-CH₃, 3H), 2.44-2.60 (O=C-CH₂, 2H), 2.17 (d, C=C-CH₂, 1H), 2.01 (d, C=C-CH₂, 1H), 1.05 (s, C-CH₃, 3H), 0.87 (s, C-

CH₃, 3H). ¹³C-NMR (125 MHz, DMSO-d₆): δ(ppm) 27.14, 28.5 29.73, 30.53, 32.63, 34.04, 50.41, 90.13, 111.72, 127.83, 129.85, 130.96, 144.24, 145.73, 150.08, 151.12, 161.294, 195.29.

Compound 4e. ¹H-NMR (500 MHz, DMSO-d₆): δ(ppm) 9.13 (s, NH, 1H), 8.01 (s, 1H, aromatic-hydrogen), 7.94 (dd, 1H, aromatic-hydrogen), 7.69 (d, 1H, aromatic-hydrogen), 7.50 (m, 1H, aromatic-hydrogen), 4.96 (s, CH, 1H), 3.44 (s, N-CH₃, 3H), 3.09 (s, N-CH₃, 3H), 2.48-2.68 (O=C-CH₂, 2H), 2.22 (d, C=C-CH₂, 1H), 2.04 (d, C=C-CH₂, 1H), 1.05 (s, C-CH₃, 3H), 0.90 (s, 3H, C-CH₃). ¹³C-NMR (125 MHz, DMSO-d₆): δ(ppm) 26.48, 28.12, 29.42, 30.68, 32.59, 34.57, 50.11, 89.83, 111.41, 121.52, 121.57, 128.53, 135.04, 144.54, 147.71, 148.97, 150.86, 150.89, 160.89, 195.30.

Compound 4k. ¹H-NMR (500 MHz, DMSO-d₆): δ (ppm) 9.08 (s, 1H, NH), 7.23 (d, 2H, aromatic-hydrogen), 6.73 (d, 2H, aromatic-hydrogen), 4.82 (s, 1H, CH), 3.66 (s, 3H, OCH₃), 3.41 (s, 3H, N-CH₃), 3.07 (s, 3H, N-CH₃), 2.55-2.65 (2H, O=C-CH₂), 2.11 (d, 1H, C=C-CH₂), 2.06 (d, 1H, C=C-CH₂), 1.03 (s, 3H, C-CH₃), 0.89 (s, 3H, C-CH₃). ¹³C-NMR (125 MHz, DMSO-d₆): δ(ppm) 26.79, 28.00, 29.73, 30.22, 32.36, 33.35, 50.64, 55.14, 90.64, 112.50, 113.44, 129.21, 139.15, 143.86, 149.37, 150.88, 151.15, 158.17, 160.92, 195.43.

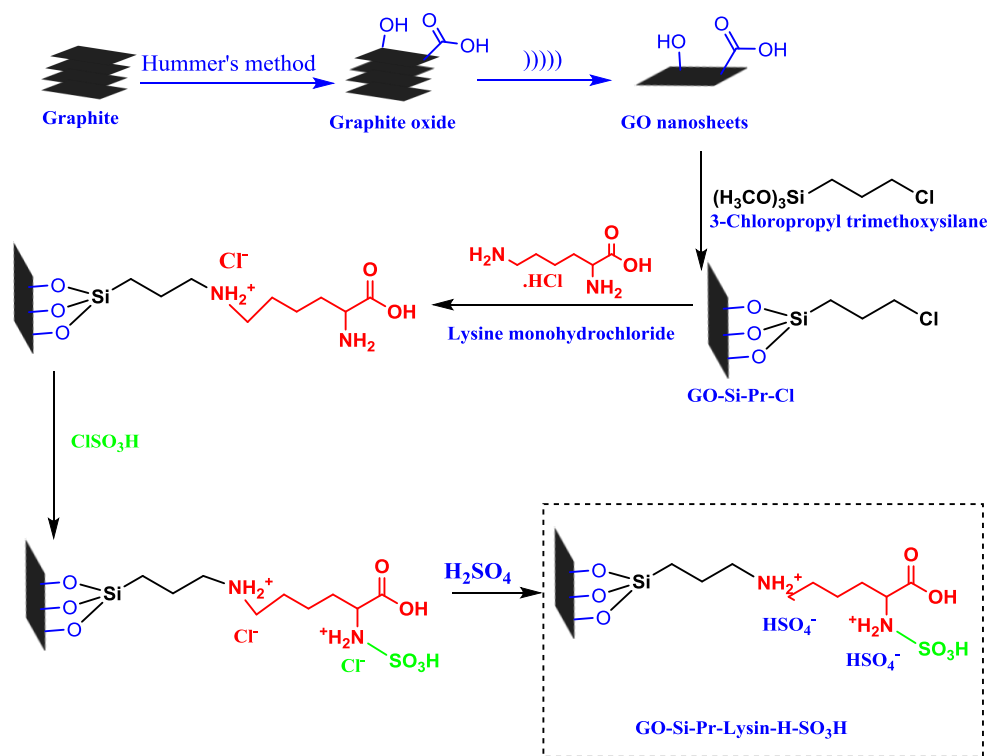
3. Results and Discussion

3.1. Preparation of the GO-Si-Pr-Lysin-SO₃H

Initially, we provided GO-Si-Pr-Lysin-SO₃H as a powerful catalyst for the application in the synthesis of pyrimido[4,5-b]quinolone derivatives (**Scheme 2**). At first, the graphene oxide nanosheets were prepared in according to the reported literature [71]. Then, 3-chloropropyltrimethoxysilane was anchored on the surface of graphene oxide nanosheets. In this step, using Mohr's method, the total density of chlorine atom were approximately measured 1.25 mmol.g⁻¹. Then, the amino acid lysine monohydrochloride was supported on the GO-Si-Pr-Cl. Finally, through the two sequential steps (**I**: addition of ClSO₃H **II**: addition of H₂SO₄), the GO-Si-Pr-Lysin-SO₃H was successfully obtained. The details of the experimental preparation of the catalyst were described in the experimental part.

3.2. Characterization of the GO-Si-Pr-Lysin-SO₃H

FT-IR technique was used for the analysis of GO, lysine-GO, and GO-Si-Pr-Lysin-SO₃H (**Fig. 2**). As can be seen in **Fig. 2**, the transmittance peak at about 1581 cm⁻¹ is related to C=C. A result of the asymmetry of GO is that the pointed peak is even sharper than graphite powder. The spectrum depicted in **Fig. 2a** exhibits peaks



Scheme 2. The general approach for the providing of GO-Si-Pr-Lysin-SO₃H

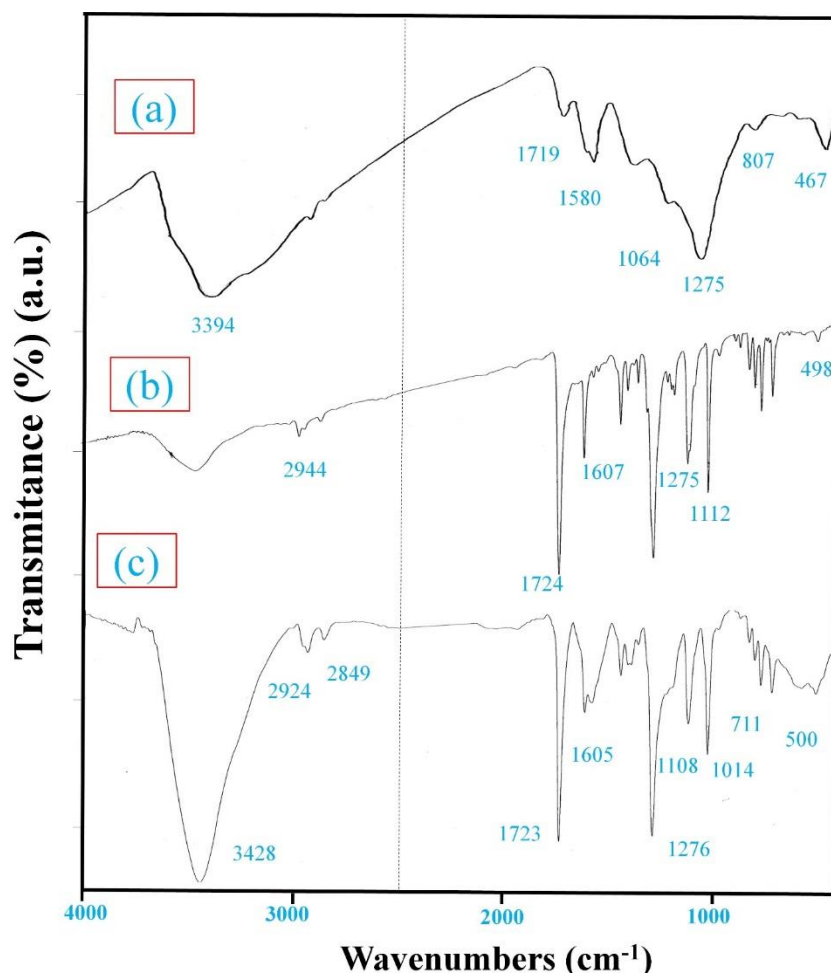


Fig. 2. FT-IR spectra of a) graphene oxide b) GO-Si-Pr-Lysin-Cl c) GO-Si-Pr-Lysin-SO₃H

at 1064, 1719, 1275, 807, 467, and 3394 cm^{-1} , which could be associated with the stretching modes of various groups attached to GO, such as C-O, C=O (carbonyl), and O-H (hydroxyl). The detection confirmed that the nitrogen-hydrogen bond bending and stretching frequencies of lysine monohydrochloride amino acid are located at $\sim 3310\text{cm}^{-1}$ and 960cm^{-1} [72]. The bands as 1722 cm^{-1} were related to C=O of carboxylic acid. In addition, it could be well observed that the lysine-monohydrochloride was successfully supported on the surface of GO through a covalent bond (Fig. 2c).

Fig. 3 displays SEM images of graphene oxide and GO-Si-Pr-Lysin-SO₃H catalyst. The FE-SEM image of GO shows the exfoliated and layered graphene oxide sheets. The morphology of GO-Si-Pr-Lysin-SO₃H was clearly converted relative to pristine GO.

Fig. 4 presents TEM images of graphene oxide and GO-Si-Pr-Lysin-SO₃H, displaying exfoliated, 2D nanostructures with large, flat, and smooth flake-like morphology. It is evident that the pristine graphite's two-dimensional flake-like shape is maintained in the graphene oxide and GO-Si-Pr-Lysin-SO₃H nanosheets even after the preparation steps of the catalyst.

Fig. 5 displays the XRD patterns of GO and GO-Si-Pr-Lysin-SO₃H. According to Hummer's method, the peak at approximately $2\theta = 26.5^\circ$ is a broad peak (in graphite powder), and the peak at $2\theta = 12^\circ$ appeared [73]. After the functionalization of graphene oxide with amino acid lysine and support of ionic liquid, the crystallinity of graphene oxide remained (Fig. 5b).

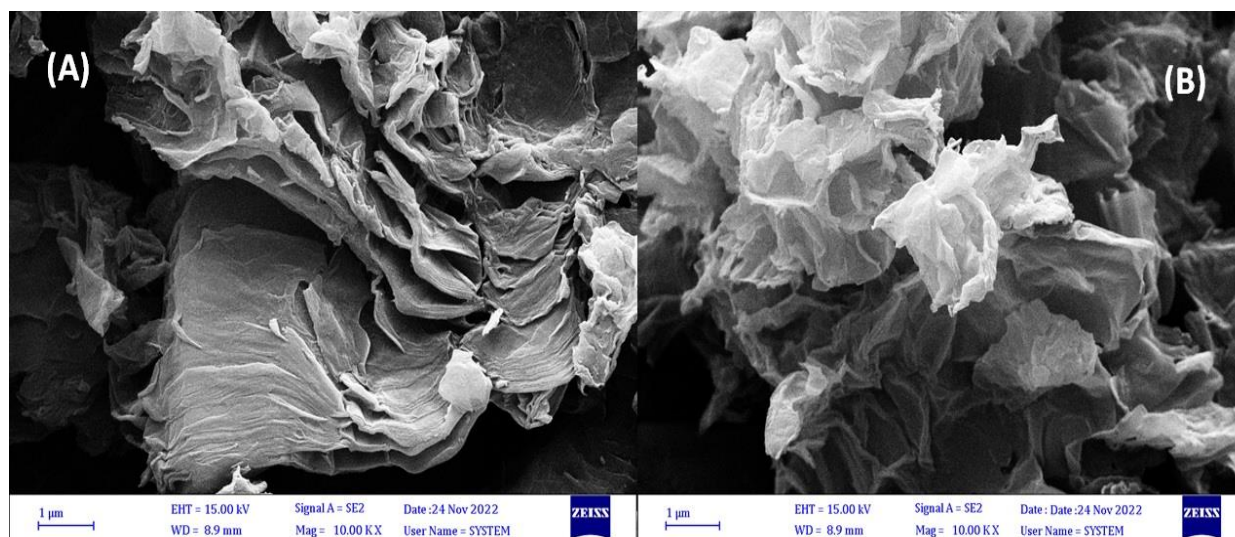


Fig. 3. FE-SEM images of a) GO b) GO-Si-Pr-Lysin-SO₃H

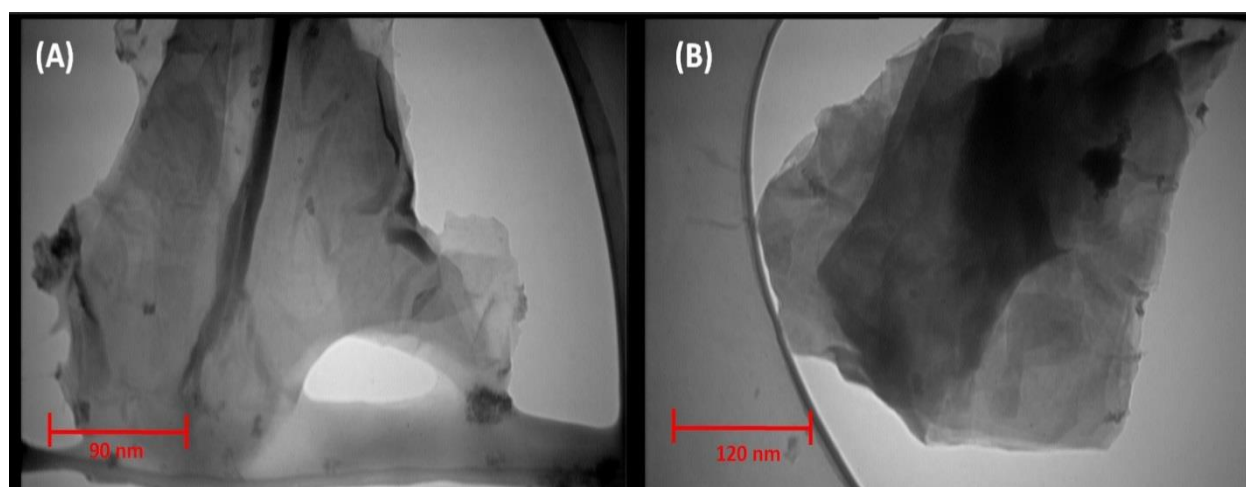


Fig. 4. TEM images of a) graphene oxide b) GO-Si-Pr-Lysin-SO₃H

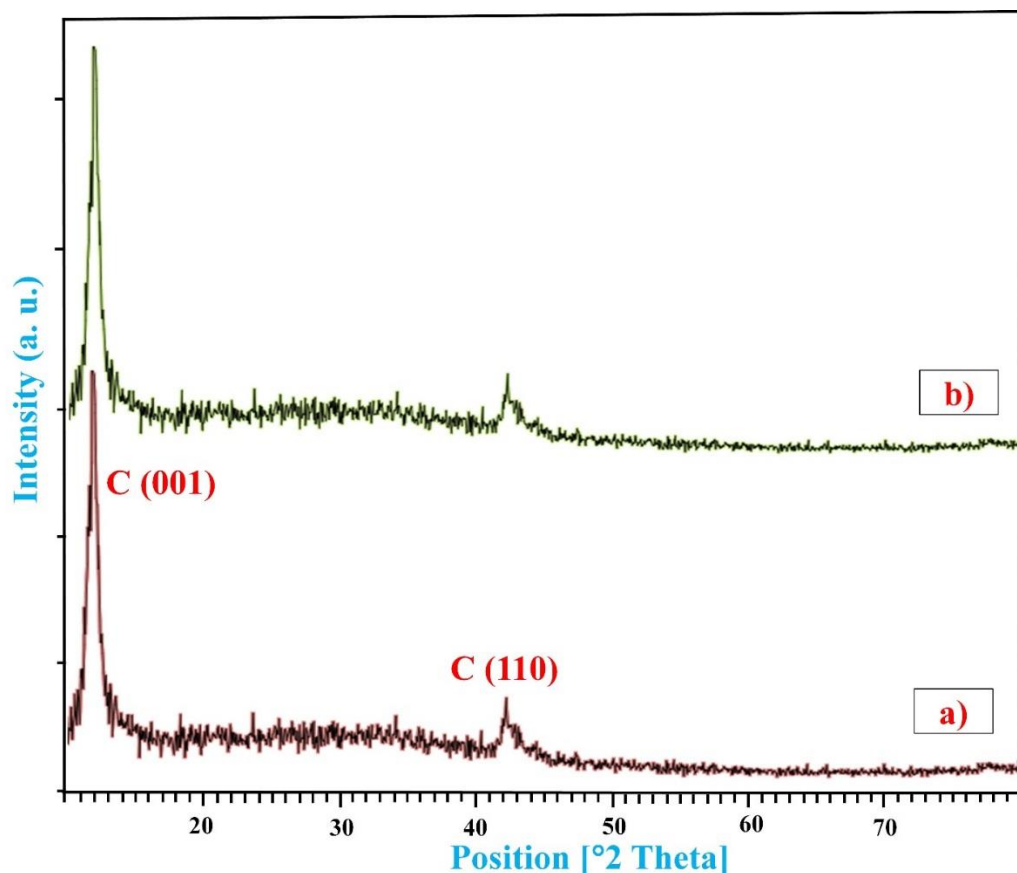


Fig. 5. XRD pattern of a) GO nanosheets and b) GO-Si-Pr-Lysin-SO₃H

Fig. 6 shows the TGA thermogram of GO-Si-Pr-Lysin-SO₃H. The TGA analysis of GO-Si-Pr-Lysin-SO₃H shows several weight decreases. The first one is attributed to trapped H₂O in the building of GO-Si-Pr-Lysin-SO₃H (65.2 °C, 4.6%). The 2nd and 3rd ones are observed at 212-313 °C, and they attributed to the

decomposition of functionalized groups (7.13% & 3.52%). Based on the TGA spectrum, the TGA thermogram shows the good thermal stability of GO-Si-Pr-Lysin-SO₃H. The later decreasing weight is related to the destruction of graphene sheets at ~445 °C (7.79%).

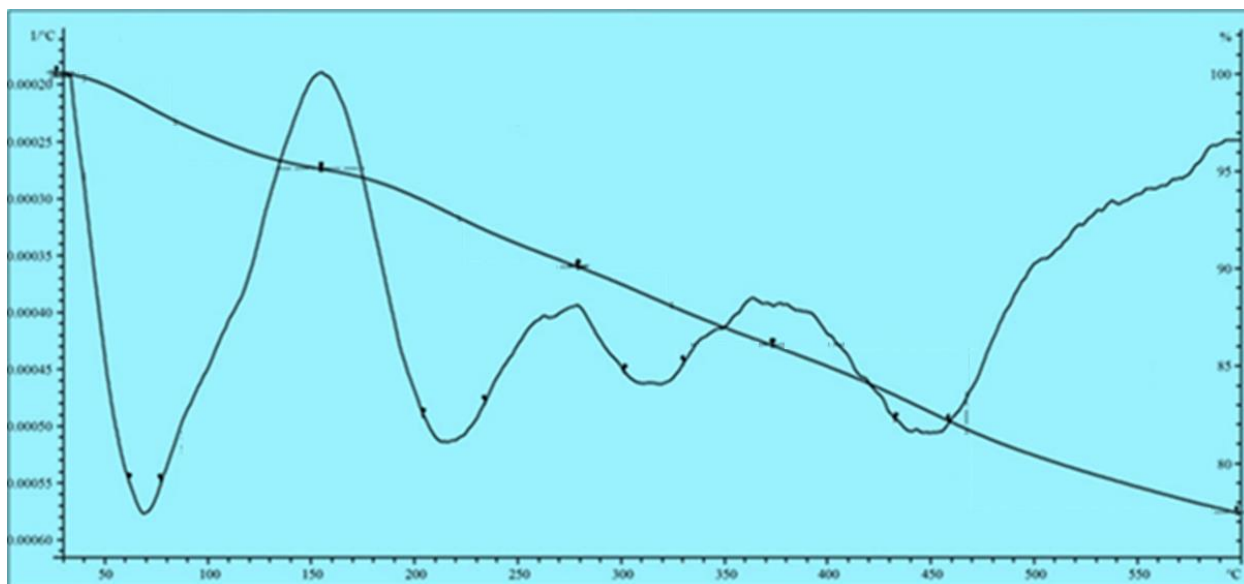


Fig. 6. TGA thermogram of GO-Si-Pr-Lysin-SO₃H

3.3. Catalytic application of GO-Si-Pr-Lysin-SO₃H

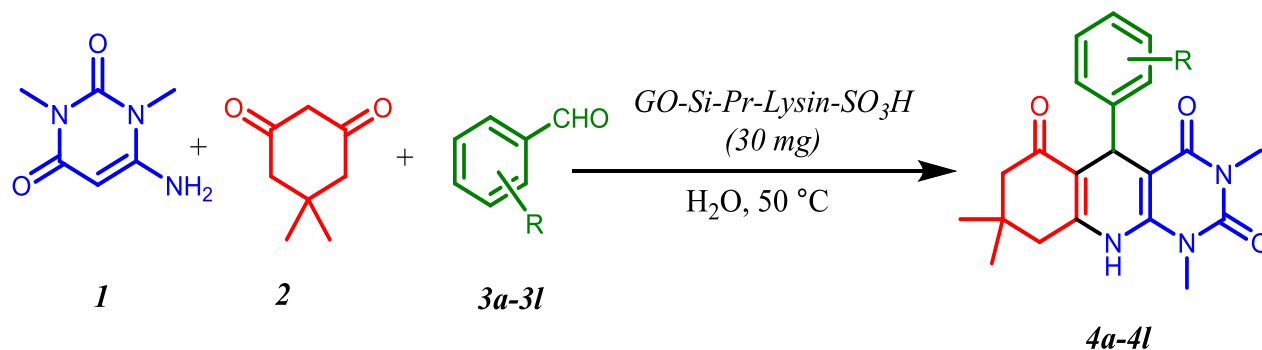
After providing and characterization of GO-Si-Pr-Lysin-SO₃H, the following reaction was performed for catalytic measurement of GO-Si-Pr-Lysin-SO₃H. The GO-Si-Pr-Lysin-SO₃H catalyzed reaction between 6-amino-1,3-dimethyluracil (**1**), dimedone (**2**), and various aromatic aldehydes (**3a-3l**) to obtain excellent pure products of pyrimido[4,5-b]quinolone derivatives in water at 50 °C (**Scheme 3**).

The reaction between 6-amino-1,3-dimethyluracil (**1**), dimedone (**2**), and benzaldehyde (**3a**) was selected as a model reaction in order to investigate the effects of temperature, solvents, and amount of GO-Si-Pr-Lysin-SO₃H. As can be seen in **Table 1**, different solvents, including ethanol, methanol, acetonitrile, water, and neat (no solvent) conditions, were chosen for evaluation of the medium reaction (**Table 1**, entries 1-5). The H₂O was selected as a good solvent for the reaction. Furthermore, altering the reaction temperature resulted in a modification of the reaction time, ultimately leading to the selection of 50°C as the optimal temperature (**Table 1**, entries 6-9). The catalytic amount of GO-Si-Pr-Lysin-SO₃H was also investigated (**Table 1**, entries 10-12). The amount of GO-Si-Pr-Lysin-SO₃H was selected as 30 mg. In these tests, entry 11 was the excellent condition for the preparation of pyrimido[4,5-b]quinolone derivatives. In order to show the efficiency of the support (graphene oxide), the ionic liquid (Lysine-H-SO₃H) was applied in the model reaction (**Table 1**, entries 13-14). However, the obtained results show that the presence of support has an effective role in the designed catalyst. Furthermore, the graphene oxide without ionic liquid was used (**Table 1**, entries 15-16). But the obtained results show that the presence of ionic liquids for the promotion of the reaction is necessary. In addition, in order to show the efficiency of

the treatment of H₂SO₄ with a catalyst (dual acidic catalyst), the GO-Si-Pr-Lys-H-Cl (before treatment of H₂SO₄) was applied in the model reaction. Our observation shows that the presence of a dual acidic catalyst was more effective in the yield and time of the reaction.

With optimization conditions in hand, several derivatives of pyrimido[4,5-b]quinolone were provided in the presence of GO-Si-Pr-Lysin-SO₃H (30 mg) (0.002 mol%) at 50 °C in water (**Table 2**). As can be seen in **Table 2**, all of the target products were produced using GO-Si-Pr-Lysin-SO₃H in good to excellent yields. Aldehydes containing electron-withdrawing (EW) groups at the o- or p- positions exhibit a reduction in reaction time and an increase in the yield of desired products, as opposed to those with electron-donating groups in the same positions. In addition, the turnover number (TON) and turnover frequency (TOF) of GO-Si-Pr-Lysin-SO₃H were changed (68.8-78.4) and (104.2-313.6), respectively.

To investigate the reusability and recyclability of GO-Si-Pr-Lysin-SO₃H, the reaction of 6-amino-1,3-dimethyluracil (**1**), dimedone (**2**), and 2,4-dichlorobenzaldehyde (**3f**), and 30 mg of GO-Si-Pr-Lysin-SO₃H was applied. The recycled catalyst was reused for six catalytic cycles (**Fig. 7**). As can be seen, a slight deactivation was observed that this event could be attributed to the washing of GO-Si-Pr-Lysin-SO₃H during the recycling procedure. Furthermore, to demonstrate the robustness of the current catalytic system, we assessed the acidity strength by conducting a back acid-base titration on both the initial and reused catalyst. Our findings indicate that the fresh catalyst exhibited a total of 2.5 mmol.g⁻¹ of active sites, while the reused catalyst (run 6th) displayed a slightly lower amount of 2.36 mmol.g⁻¹.



Scheme 3. Preparation of pyrimido[4,5-b]quinolone derivatives using GO-Si-Pr-Lysin-SO₃H in water

Table 1. Optimization of the reaction conditions

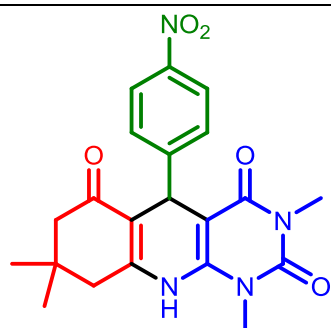
Reaction scheme: 1 + 2 + 3a $\xrightarrow{\text{Catalyst}}$ 4a

Entry	Type of Catalyst	Catalyst (mg)	Solvent	T (°C)	Time (min)	Yield (%) ^a
1	GO-Si-Pr-Lysin-H-SO ₃ H	20	EtOH	Reflux	60	40
2	GO-Si-Pr-Lysin-H-SO ₃ H	20	MeOH	Reflux	60	45
3	GO-Si-Pr-Lysin-H-SO ₃ H	20	CH ₃ CN	Reflux	60	35
4	GO-Si-Pr-Lysin-H-SO ₃ H	20	H ₂ O	Reflux	60	70
5	GO-Si-Pr-Lysin-H-SO ₃ H	20	Solvent-free	90	60	25
6	GO-Si-Pr-Lysin-H-SO ₃ H	20	H ₂ O	80	60(25) ^b	70
7	GO-Si-Pr-Lysin-H-SO ₃ H	20	H ₂ O	60	25	70
8	GO-Si-Pr-Lysin-H-SO ₃ H	20	H ₂ O	50	25	70
9	GO-Si-Pr-Lysin-H-SO ₃ H	20	H ₂ O	40	70	55
10	GO-Si-Pr-Lysin-H-SO ₃ H	25	H ₂ O	50	25	80
11	GO-Si-Pr-Lysin-H-SO ₃ H	30	H ₂ O	50	25	92
12	GO-Si-Pr-Lysin-H-SO ₃ H	35	H ₂ O	50	25	88
13	Lysine-H-SO ₃ H	40 (~0.5 mL)	Net.	50	60	50
14	Lysine-H-SO ₃ H	40 (~0.5 mL)	Net.	100	60	65
15	Graphene Oxide	50	H ₂ O	Reflux	120	35
16	Graphene Oxide	50	Solvent-free	80	180	35
17	GO-Si-Pr-Lys-H-Cl (before treatment of H ₂ SO ₄)	50	H ₂ O	50	60	50

a: Isolated Yields. b: The time of the reaction was followed until 60 min. But after 25 min, no specific development was observed.

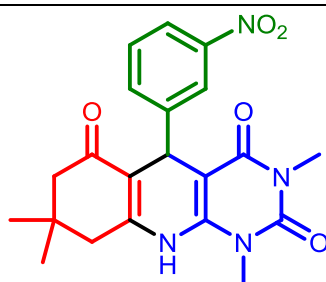
Table 2. Synthesis of pyrimido[4,5-b]quinolone derivatives using GO-Si-Pr-Lysin-SO₃H in water^a

4a-4l		
<hr/>		
<p>4a</p> <p>Yield:^b 92% Time:^c 25 TON:^d 73.6 TOF (h⁻¹):^e 176.5</p>	<p>4b</p> <p>Yield: 96% Time: 15 TON: 76.8 TOF (h⁻¹): 307.2</p>	<p>4c</p> <p>Yield: 95% Time: 18 TON: 76 TOF (h⁻¹): 316.7</p>
<hr/>		
<p>4d</p> <p>Yield: 97% Time: 20 TON: 77.6 TOF (h⁻¹): 235.1</p>	<p>4e</p> <p>Yield: 93% Time: 22 TON: 74.4 TOF (h⁻¹): 203.3</p>	<p>4f</p> <p>Yield: 98% Time: 15 TON: 78.4 TOF (h⁻¹): 313.6</p>



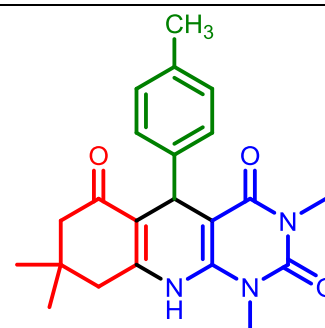
4g

Yield: 94%
Time: 18
TON: 75.2
TOF (h⁻¹): 250.7



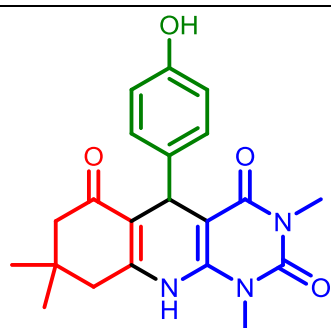
4h

Yield: 92%
Time: 22
TON: 73.6
TOF (h⁻¹): 223.0



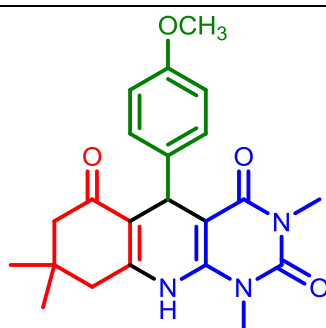
4i

Yield: 90%
Time: 33
TON: 72
TOF (h⁻¹): 130.9



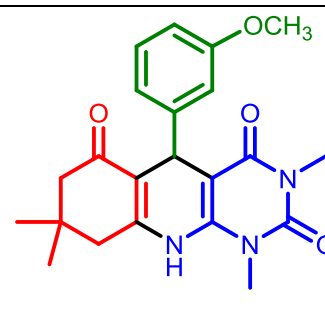
4j

Yield: 89%
Time: 40
TON: 71.2
TOF (h⁻¹): 107.9



4k

Yield: 86%
Time: 40
TON: 68.8
TOF (h⁻¹): 104.2



4l

Yield: 87%
Time: 40
TON: 69.6
TOF (h⁻¹): 105.4

- a) General reaction conditions: 6-Amino-1,3-dimethyluracil (1) (1 mmol), dimedone (2) (1 mmol), aromatic aldehyde (3a-3l) (1 mmol), T: 50 °C, H₂O: 3 mL, Catalyst: 30 mg (0.002 mol%).
b) Isolated Yields.
c) Time of the reaction was reported as minutes.
d) TON (Turnover number): (mmol of the desired product per mmol of the active sites on the surface of the catalyst)
e) TOF (Turnover frequency): (TON per time of the reaction as hour).

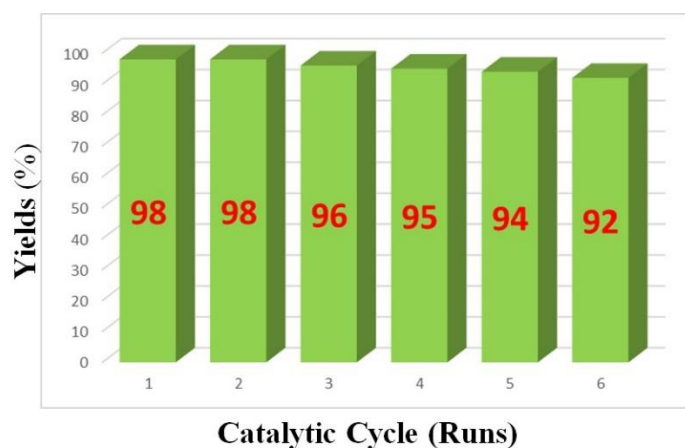
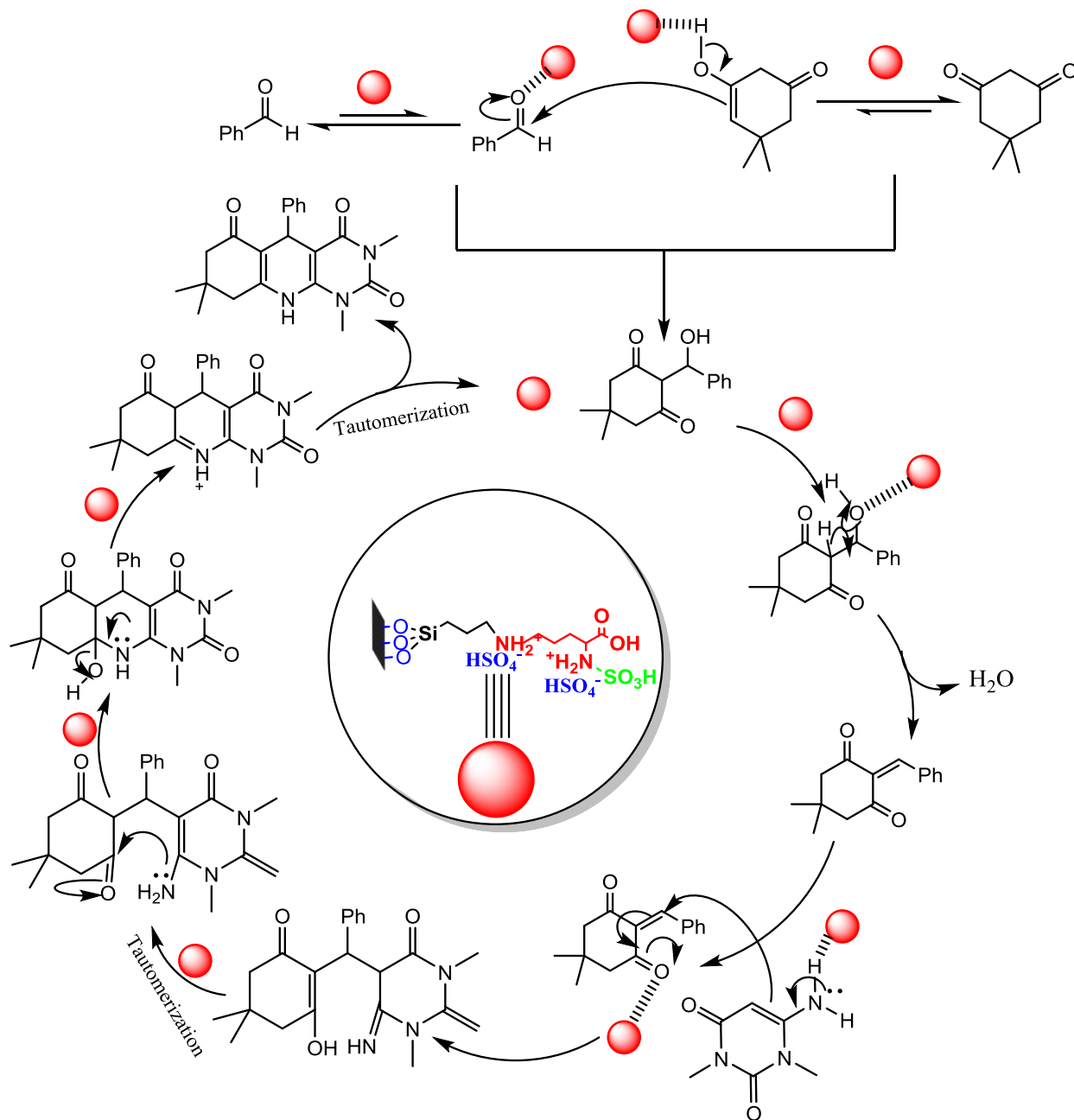


Fig. 7. The reusability of the GO-Si-Pr-Lysin-SO₃H for the synthesis of product **4f** within 15 min.

As can be previously introduced, GO-Si-Pr-Lysin-SO₃H was a dual acidic ionic liquid including two hydrogen sulfate as anion and one sulfonic acid group. Therefore, the designed catalyst could be applied for both acidic and basic organic reactions. The roles of GO-Si-Pr-Lysin-SO₃H was shown in **Scheme 4**. In the first step, the acidic hydrogen of sulfonic acid or hydrogen sulfate have activated the carbonyl groups in aldehydes and dimedone. Therefore, the carbon of carbonyl groups was appropriate for nucleophilic attacks. Then, the catalyst promoted the removal of water from intermediate

molecules. In addition, the GO-Si-Pr-Lysin-SO₃H catalyzed the tautomerization process in the two steps.

In order to check the efficiency of GO-Si-Pr-Lysin-SO₃H be compared with previously reported catalysts, the synthesis of compound **4a** were selected and compared in specific keywords, including amount of catalyst, reaction conditions, time, yield, and TOF of the catalyst (**Table 3**). As can be seen, the efficiency of GO-Si-Pr-Lysin-SO₃H was highlighted in less reaction time, more yield of the reaction, and mild reaction conditions.



Scheme 4. The suggested reaction mechanism

Table 3. Result comparison of GO-Si-Pr-Lysin-SO₃H with other previous reported catalyst in the synthesis of 4a

Entry	Catalyst name	Amount (mol%)	Conditions	Time (min)	Yield (%)	TOF	Ref.
1	1-Butyl-3-methylimidazolium bromide ([bmim]Br)	2 mL	95 °C/Solvent-free	210	90	--	[74]
2	Cellulose-SO ₃ H	0.06 g	90 °C/Solvent-free	30	96	--	[75]
3	InCl ₃	0.2	Reflux/ H ₂ O	60	91	0.13	[76]
4	<i>p</i> -Ts-SO ₃ H	0.2	90 °C/ H ₂ O	150	89	0.049	[77]
5	Fe ₃ O ₄ -SiO ₂ -SO ₃ H	0.02 g	70 °C/ H ₂ O	25	92	--	[78]
6	1,3-DiSO ₃ H-Imid-HSO ₄	2.5 × 10 ⁻⁴	70 °C/ EtOH	15	91	404.44	[79]
7	[H ₂ -DABCO][H ₂ PO ₄] ₂	2.3 × 10 ⁻⁴	75 °C/ H ₂ O: EtOH (2:1)	240	Not completed	---	[80]
8	[H ₂ -DABCO][HSO ₄] ₂	1.6 × 10 ⁻⁴	75 °C/ H ₂ O: EtOH (2:1)	70	93	138.39	[80]
9	GO-Si-Pr-Lysin-SO ₃ H	0.002	50 °C/ H ₂ O	20	97	176.5	This work

4. Conclusions

In summary, in this study, we have described a novel and powerful dual acidic ionic liquid supported on graphene oxide nanosheets (GO-Si-Pr-Lysin-SO₃H) for the preparation of pyrimido[4,5-b]quinolone derivatives. This methodology has several advantages, including excellent yields of the target products, short reaction times, and reusability of the catalyst, green and eco-friendly solvent, and simple purification of the catalyst.

Acknowledgements

The authors acknowledge for the financial support of Mosul University for supporting of this study.

References

- [1] Y. Abouelhasan, A.T. Garrison, G.M. Burch, W. Wong, V.M. Norwood IV, R.W. Huigens III, Discovery of quinoline small molecules with potent dispersal activity against methicillin-resistant *Staphylococcus aureus* and *Staphylococcus epidermidis* biofilms using a scaffold hopping strategy, *Bioorg. Med. Chem. Lett.*, 24 (2014) 5076-5080.
- [2] Y. Abouelhasan, A.T. Garrison, F. Bai, V.M. Norwood IV, M.T. Nguyen, S. Jin, R.W. Huigens III, A phytochemical-halogenated quinoline combination therapy strategy for the treatment of pathogenic bacteria, *ChemMedChem*, 10 (2015) 1157-1162.
- [3] M.A.A. Al-Bari, Chloroquine analogues in drug discovery: new directions of uses, mechanisms of actions and toxic manifestations from malaria to multifarious diseases, *J. Antimicrob. Chemother.*, 70 (2015) 1608-1621.
- [4] I. Aleksić, S. Šegan, F. Andric, M. Zlatović, I. Moric, D.M. Opsenica, L. Senerovic, Long-chain 4-aminoquinolines as quorum sensing inhibitors in *Serratia marcescens* and *Pseudomonas aeruginosa*, *ACS Chem. Biol.*, 12 (2017) 1425-1434.
- [5] F. Jalili, M. Zarei, M.A. Zolfigol, S. Rostamnia, A.R. Moosavi-Zare, SBA-15/PrN (CH₂PO₃H₂)₂ as a novel and efficient mesoporous solid acid catalyst with phosphorous acid tags and its application on the synthesis of new pyrimido [4, 5-b] quinolones and pyrido [2, 3-d] pyrimidines via anomeric based oxidation, *Microporous Mesoporous Mater.*, 294 (2020) 109865.
- [6] F. Shirini, M.S.N. Langarudi, N. Daneshvar, N. Jamasbi, M. Irankhah-Khanghah, Preparation and characterization of [H₂-DABCO][ClO₄]₂ as a new member of DABCO-based ionic liquids for the synthesis of pyrimido [4, 5-b]-quinoline and pyrimido [4, 5-d] pyrimidine derivatives, *J. Mol. Struct.*, 1161 (2018) 366-382.
- [7] F. Shirini, M.S.N. Langarudi, N. Daneshvar, M. Mashhadinezhad, N. Nabinia, Preparation of a new DABCO-based ionic liquid and investigation on its application in the synthesis of

benzimidazoquinazolinone and pyrimido [4, 5-b]-quinoline derivatives, *J. Mol. Liq.*, 243 (2017) 302-312.

[8] H. Sepehrmansouri, M. Zarei, M.A. Zolfigol, A.R. Moosavi-Zare, S. Rostamnia, S. Moradi, Multilinker phosphorous acid anchored En/MIL-100 (Cr) as a novel nanoporous catalyst for the synthesis of new N-heterocyclic pyrimido [4, 5-b] quinolines, *Molecular Catalysis*, 481 (2020) 110303.

[9] A.K. Panday, R. Mishra, A. Jana, T. Parvin, L.H. Choudhury, Synthesis of pyrimidine fused quinolines by ligand-free copper-catalyzed domino reactions, *J. Org. Chem.*, 83 (2018) 3624-3632.

[10] F. Osanlou, F. Nemati, S. Sabaqian, An eco-friendly and magnetized biopolymer cellulose-based heterogeneous acid catalyst for facile synthesis of functionalized pyrimido [4, 5-b] quinolines and indeno fused pyrido [2, 3-d] pyrimidines in water, *Res. Chem. Intermed.*, 43 (2017) 2159-2174.

[11] D.M. Patel, H.J. Patel, J.M. Padrón, H.M. Patel, A novel substrate directed multicomponent reaction for the syntheses of tetrahydro-spiro [pyrazolo [4, 3-f] quinoline]-8, 5'-pyrimidines and tetrahydro-pyrazolo [4, 3-f] pyrimido [4, 5-b] quinolines via selective multiple C-C bond formation under metal-free conditions, *RSC Adv.*, 10 (2020) 19600-19609.

[12] A. Zare, N. Lotfifar, M. Dianat, Preparation, characterization and application of nano-[Fe₃O₄@-SiO₂@ R-NHMe₂][H₂PO₄] as a novel magnetically recoverable catalyst for the synthesis of pyrimido [4, 5-b] quinolines, *J. Mol. Struct.*, 1211 (2020) 128030.

[13] A. Zare, M. Dianat, M.M. Eskandari, A novel organic-inorganic hybrid material: production, characterization and catalytic performance for the reaction of arylaldehydes, dimedone and 6-amino-1, 3-dimethyluracil, *New J. Chem.*, 44 (2020) 4736-4743.

[14] R. Singha, P. Basak, M. Bhattacharya, P. Ghosh, Graphene oxide catalyzed one-pot synthesis of pyrimido [4, 5-b] quinolinone-2, 4-diones and their biological evaluation, *ChemistrySelect*, 5 (2020) 6514-6525.

[15] S.S. Reddy, M.V.K. Reddy, P.V.G. Reddy, β-Cyclodextrin in Water: As an Efficient Green Protocol for the Synthesis of Pyrimido [4, 5-b] quinoline-diones, *ChemistrySelect*, 3 (2018) 4283-4288.

[16] A. Gholami, M. Mokhtary, M. Nikpassand, Glycolic acid-supported cobalt ferrite-catalyzed one-pot synthesis of pyrimido [4, 5-b] quinoline and indenopyrido [2, 3-d] pyrimidine derivatives, *Appl. Organomet. Chem.*, 34 (2020) e6007.

[17] A. Zare, M. Barzegar, Dicationic ionic liquid grafted with silica-coated nano-Fe₃O₄ as a novel and efficient catalyst for the preparation of uracil-containing heterocycles, *Res. Chem. Intermed.*, 46 (2020) 3727-3740.

[18] J. Safari, M. Tavakoli, M.A. Ghasemzadeh, A highly effective synthesis of pyrimido [4, 5-b] quinoline-tetraones using H₃PW₁₂O₄₀/chitosan/NiCo₂O₄ as a novel magnetic nanocomposite, *Polyhedron*, 182 (2020) 114459.

[19] F. Jalili, M. Zarei, M.A. Zolfigol, A. Khazaei, Application of novel metal-organic framework [Zr-UiO-66-PDC-SO₃H] FeCl₄ in the synthesis of dihydrobenzo [g] pyrimido [4, 5-b] quinoline derivatives, *RSC Adv.*, 12 (2022) 9058-9068.

[20] A. Zare, M. Dianat, A highly efficient and green approach for the synthesis of pyrimido [4, 5-b] quinolines using N, N-diethyl-N-sulfoethanaminium chloride, *Zeitschrift für Naturforschung B*, 76 (2021) 85-90.

[21] M. Mamaghani, M. Jamali Moghadam, R. Hossein Nia, A facile ZrO₂ nanoparticles catalyzed synthesis of 2-amino-5-arylpymido [4, 5-b] quinolinediones, *J. Iran. Chem. Soc.*, 14 (2017) 395-401.

[22] J.B. Singh, K. Mishra, T. Gupta, R.M. Singh, Copper-catalyzed cascade reaction: synthesis of pyrimido [4, 5-b] quinolinones from 2-chloroquinoline-3-carbonitriles with (aryl) methanamines, *New J. Chem.*, 42 (2018) 3310-3314.

[23] A.R. Moosavi-Zare, H. Goudarziafshar, Z. Bahrami, Nano-[Cu-4C₃NSP](Cl)₂ as a new catalyst for the preparation of pyrimido [4, 5-b] quinoline derivatives, *Res. Chem. Intermed.*, (2022) 1-17.

[24] S. Esmaili, A.R. Moosavi-Zare, A. Khazaei, Z. Najafi, Synthesis of Novel Pyrimido [4, 5-b] Quinolines Containing Benzyloxy and 1, 2, 3-Triazole Moieties by DABCO as a Basic Catalyst, *ACS omega*, 7 (2022) 45314-45324.

[25] L. Edjlali, R.H. Khanamiri, J. Abolhasani, Fe₃O₄ nano-particles supported on cellulose as an efficient catalyst for the synthesis of pyrimido [4, 5-b] quinolines in water, *Monatshefte für Chemie-Chemical Monthly*, 146 (2015) 1339-1342.

[26] N.A. Hassan, M.I. Hegab, F. Abdel-Motti, S. Hebah, F. Abdel-Megeid, A. Hashem, Three-component, one-pot synthesis of pyrimido [4, 5-b]-quinoline and pyrido [2, 3-d] pyrimidine derivatives, *J. Heterocycl. Chem.*, 44 (2007) 775-782.

- [27] G.K. Verma, K. Raghuvanshi, R. Kumar, M.S. Singh, An efficient one-pot three-component synthesis of functionalized pyrimido [4, 5-b] quinolines and indeno fused pyrido [2, 3-d] pyrimidines in water, *Tetrahedron Lett.*, 53 (2012) 399-402.
- [28] S.J. Ji, S.N. Ni, F. Yang, J.W. Shi, G.L. Dou, X.Y. Li, X.S. Wang, D.Q. Shi, An Efficient synthesis of pyrimido [4, 5-b] quinoline and indeno [2', 1': 5, 6] pyrido [2, 3-d] pyrimidine derivatives via multicomponent reactions in ionic liquid, *J. Heterocycl. Chem.*, 45 (2008) 693-702.
- [29] K. Mohammadi, F. Shirini, A. Yahyazadeh, 1, 3-Disulfonic acid imidazolium hydrogen sulfate: a reusable and efficient ionic liquid for the one-pot multicomponent synthesis of pyrimido [4, 5-b] quinoline derivatives, *RSC Adv.*, 5 (2015) 23586-23590.
- [30] K. Tabatabaeian, A.F. Shojaei, F. Shirini, S.Z. Hejazi, M. Rassa, A green multicomponent synthesis of bioactive pyrimido [4, 5-b] quinoline derivatives as antibacterial agents in water catalyzed by $\text{RuCl}_3 \cdot x\text{H}_2\text{O}$, *Chin. Chem. Lett.*, 25 (2014) 308-312.
- [31] S. Abdolmohammadi, S. Balalaie, M. Barari, F. Rominger, Three-component green reaction of arylaldehydes, 6-amino-1, 3-dimethyluracil and active methylene compounds catalyzed by $\text{Zr}(\text{HSO}_4)_4$ under solvent-free conditions, *Combinatorial Chem. High Throughput Screening*, 16 (2013) 150-159.
- [32] D. Li, R.B. Kaner, Graphene-based materials, *Science*, 320 (2008) 1170-1171.
- [33] C.e.N.e.R. Rao, A.e.K. Sood, K.e.S. Subrahmanyam, A. Govindaraj, Graphene: the new two-dimensional nanomaterial, *Angew. Chem. Int. Ed.*, 48 (2009) 7752-7777.
- [34] C. Rao, A. Sood, R. Voggu, K. Subrahmanyam, Some novel attributes of graphene, *The Journal of Physical Chemistry Letters*, 1 (2010) 572-580.
- [35] F. Gao, S. Zhang, Q. Lv, B. Yu, Recent advances in graphene oxide catalyzed organic transformations, *Chin. Chem. Lett.*, 33 (2022) 2354-2362.
- [36] S. Guo, S. Garaj, A. Bianco, C. Ménard-Moyon, Controlling covalent chemistry on graphene oxide, *Nature Reviews Physics*, 4 (2022) 247-262.
- [37] A. Jiříčková, O. Jankovský, Z. Sofer, D. Sedmidubský, Synthesis and applications of graphene oxide, *Materials*, 15 (2022) 920.
- [38] M. Verma, I. Lee, J. Oh, V. Kumar, H. Kim, Synthesis of EDTA-functionalized graphene oxide-chitosan nanocomposite for simultaneous removal of inorganic and organic pollutants from complex wastewater, *Chemosphere*, 287 (2022) 132385.
- [39] A.H. Cahyana, A.R. Liandi, M. Maghdalena, R.T. Yunarti, T.P. Wendari, Magnetically separable $\text{Fe}_3\text{O}_4/\text{graphene oxide}$ nanocomposite: an efficient heterogenous catalyst for spirooxindole derivatives synthesis, *Ceram. Int.*, 48 (2022) 18316-18323.
- [40] P. Kumar, V. Tomar, D. Kumar, R.K. Joshi, M. Nemiwal, Magnetically active iron oxide nanoparticles for catalysis of organic transformations: A review, *Tetrahedron*, (2022) 132641.
- [41] M. Mirza-Aghayan, M. Mohammadi, R. Boukherroub, Synthesis and characterization of palladium nanoparticles immobilized on graphene oxide functionalized with triethylenetetramine or 2, 6-diaminopyridine and application for the Suzuki cross-coupling reaction, *J. Organomet. Chem.*, 957 (2022) 122160.
- [42] S.F. Adil, M. Ashraf, M. Khan, M.E. Assal, M.R. Shaik, M. Kuniyil, A. Al-Warthan, M.R.H. Siddiqui, W. Tremel, M.N. Tahir, Advances in graphene/inorganic nanoparticle composites for catalytic applications, *The Chemical Record*, 22 (2022) e202100274.
- [43] N. Nandal, P.K. Prajapati, B.M. Abraham, S.L. Jain, CO_2 to ethanol: A selective photoelectrochemical conversion using a ternary composite consisting of graphene oxide/copper oxide and a copper-based metal-organic framework, *Electrochim. Acta*, 404 (2022) 139612.
- [44] S.H. Gebre, Recent developments of supported and magnetic nanocatalysts for organic transformations: an up-to-date review, *Applied Nanoscience*, 13 (2023) 15-63.
- [45] W. Li, A. Xu, Y. Zhang, Y. Yu, Z. Liu, Y. Qin, Metal-organic framework-derived Mn_3O_4 nanostructure on reduced graphene oxide as high-performance supercapacitor electrodes, *J. Alloys Compd.*, 897 (2022) 162640.
- [46] H.-M. Song, L.-J. Zhu, Y. Wang, G. Wang, Z.-X. Zeng, Fe-based Prussian blue cubes confined in graphene oxide nanosheets for the catalytic degradation of dyes in wastewater, *Sep. Purif. Technol.*, 288 (2022) 120676.
- [47] S.M.-G. Yek, M. Nasrollahzadeh, D. Azarifar, A. Rostami-Vartooni, M. Ghaemi, M. Shokouhimehr, Grafting Schiff base Cu (II) complex on magnetic graphene oxide as an efficient recyclable catalyst for the synthesis of 4H-pyrano [2, 3-b] pyridine-3-carboxylate derivatives, *Mater. Chem. Phys.*, 284 (2022) 126053.

- [48] O. Mohammadi, M. Golestanzadeh, M. Abdouss, Recent advances in organic reactions catalyzed by graphene oxide and sulfonated graphene as heterogeneous nanocatalysts: a review, *New J. Chem.*, 41 (2017) 11471-11497.
- [49] H. Naeimi, M. Golestanzadeh, Microwave-assisted synthesis of 6,6'-(aryl(alkyl)methylene)bis(2,4-dialkylphenol) antioxidants catalyzed by multi-sulfonated reduced graphene oxide nanosheets in water, *New J. Chem.*, 39 (2015) 2697-2710.
- [50] H. Naeimi, M. Golestanzadeh, Highly sulfonated graphene and graphene oxide nanosheets as heterogeneous nanocatalysts in green synthesis of bisphenolic antioxidants under solvent free conditions, *RSC Adv.*, 4 (2014) 56475-56488.
- [51] R. Fareghi-Alamdari, M. Golestanzadeh, O. Bagheri, meso-Tetrakis[4-(methoxycarbonyl)phenyl]porphyrinatopalladium(ii) supported on graphene oxide nanosheets (Pd(ii)-TMCPP-GO): synthesis and catalytic activity, *RSC Adv.*, 6 (2016) 108755-108767.
- [52] M. Golestanzadeh, H. Naeimi, Z. Zahraie, Synthesis and antioxidant activity of star-shape phenolic antioxidants catalyzed by acidic nanocatalyst based on reduced graphene oxide, *Mater. Sci. Eng., C*, 71 (2017) 709-717.
- [53] F. Panahi, R. Fareghi-Alamdari, S. Khajeh Dangolani, A. Khalafi-Nezhad, M. Golestanzadeh, Graphene Grafted N-Methyl-4-pyridinamine (G-NMPA): An Efficient Heterogeneous Organocatalyst for Acetylation of Alcohols, *ChemistrySelect*, 2 (2017) 474-479.
- [54] H. Naeimi, M. Golestanzadeh, Z. Zahraie, Synthesis of potential antioxidants by synergy of ultrasound and acidic graphene nanosheets as catalyst in water, *Int. J. Biol. Macromol.*, 83 (2016) 345-357.
- [55] R. Fareghi-Alamdari, M. Golestanzadeh, F. Agend, N. Zekri, Synthesis, characterization and catalytic activity of sulphonated multi-walled carbon nanotubes as heterogeneous, robust and reusable catalysts for the synthesis of bisphenolic antioxidants under solvent-free conditions, *J. Chem. Sci.*, 125 (2013) 1185-1195.
- [56] R. Fareghi-Alamdari, M. Golestanzadeh, F. Agend, N. Zekri, Regiospecific, one-pot, and pseudo-five-component synthesis of 6,6'-(arylmethylene)bis(2-(tert-butyl)4-methylphenol) antioxidants using highly sulfonated multi-walled carbon nanotubes under solvent-free conditions, *Can. J. Chem.*, 91 (2013) 982-991.
- [57] M. Golestanzadeh, H. Naeimi, Z. Zahraie, Metal-free GO-SiPr-SO₃H Nanosheets Catalyzed Ultrasound Promoted One-pot Synthesis of Star-Shape Phenolic Compounds in Water and Study of Their In-vitro Antimicrobial Activities, *ChemistrySelect*, 1 (2016) 6490-6498.
- [58] M. Golestanzadeh, H. Naeimi, Palladium decorated on a new dendritic complex with nitrogen ligation grafted to graphene oxide: fabrication, characterization, and catalytic application, *RSC Adv.*, 9 (2019) 27560-27573.
- [59] R. Fareghi-Alamdari, M. Golestanzadeh, N. Zekri, Solvent-free synthesis of trisphenols as starting precursors for the synthesis of calix[4]arenes using sulfonated multi-walled carbon nanotubes, *New J. Chem.*, 40 (2016) 3400-3412.
- [60] R. Fareghi-Alamdari, M. Golestanzadeh, N. Zekri, Z. Mavedatpoor, Multi SO₃H supported on carbon nanotubes: a practical, reusable, and regioselective catalysts for the tert-butylation of p-cresol under solvent-free conditions, *J. Iran. Chem. Soc.*, 12 (2015) 537-549.
- [61] M. Golestanzadeh, H. Naeimi, Effect of Confined Spaces in the Catalytic Activity of 1D and 2D Heterogeneous Carbon-Based Catalysts for Synthesis of 1,3,5-Triarylbenzenes: RGO-SO₃H vs. MWCNTs-SO₃H, *ChemistrySelect*, 4 (2019) 1909-1921.
- [62] O. Mohammadi, M. Golestanzadeh, M. Abdouss, Metal-Free and Ultrasound-Assisted C-C and O-Si (O-Protected) Bond Formation in Cyanosilylation of Aldehydes with TMSCN Catalyzed by Functionalized Graphene Oxide Derivatives, *ChemistrySelect*, 3 (2018) 12131-12138.
- [63] X. Tang, S. Lv, K. Jiang, G. Zhou, X. Liu, Recent development of ionic liquid-based electrolytes in lithium-ion batteries, *J. Power Sources*, 542 (2022) 231792.
- [64] C.S. Buettner, A. Cognigni, C. Schroeder, K. Bica-Schröder, Surface-active ionic liquids: A review, *J. Mol. Liq.*, 347 (2022) 118160.
- [65] T.M. Dhameliya, P.R. Nagar, K.A. Bhakhar, H.R. Jivani, B.J. Shah, K.M. Patel, V.S. Patel, A.H. Soni, L.P. Joshi, N.D. Gajjar, Recent advancements in applications of ionic liquids in synthetic construction of heterocyclic scaffolds: A spotlight, *J. Mol. Liq.*, 348 (2022) 118329.
- [66] M. Kazemi, L. Shiri, Ionic liquid immobilized on magnetic nanoparticles: a nice and efficient catalytic strategy in synthesis of heterocycles, *Journal of Synthetic Chemistry*, 1 (2022) 1-7.

- [67] G. Li, S. Dong, P. Fu, Q. Yue, Y. Zhou, J. Wang, Synthesis of porous poly (ionic liquid) s for chemical CO₂ fixation with epoxides, *Green Chem.*, 24 (2022) 3433-3460.
- [68] A.H. Ali, M.Y. Saleh, K.A. Owaed, Mild Synthesis, Characterization, and Application of some Polythioester Polymers Catalyzed by Cetrinide Ionic Liquid as a Green and Eco-Friendly Phase-Transfer Catalyst, *Iran. J. Catal.*, 13 (2023) 73-83.
- [69] A.M. Hamdoon, M.Y. Saleh, S.M. Saied, Synthesis & Biological Evaluation of Novel Series of Benzo [f] indazole Derivatives, *Egyptian Journal of Chemistry*, 65 (2022) 305-312.
- [70] S.M. Saied, M.Y. Saleh, A.M. Hamdoon, Multicomponent Synthesis of Tetrahydrobenzo [a] xanthene and Tetrahydrobenzo [a] acridine Derivatives using Sulfonated Multi-Walled Carbon Nanotubes as Heterogeneous Nanocatalysts, *Iran. J. Catal.*, 12 (2022) 189-205.
- [71] N. Zaaba, K. Foo, U. Hashim, S. Tan, W.-W. Liu, C. Voon, Synthesis of graphene oxide using modified hummers method: solvent influence, *Procedia engineering*, 184 (2017) 469-477.
- [72] K. Prendergast, T.G. Spiro, Core expansion, ruffling, and doming effects on metalloporphyrin vibrational frequencies, *J. Am. Chem. Soc.*, 114 (1992) 3793-3801.
- [73] D. Long, W. Li, L. Ling, J. Miyawaki, I. Mochida, S.-H. Yoon, Preparation of nitrogen-doped graphene sheets by a combined chemical and hydrothermal reduction of graphene oxide, *Langmuir*, 26 (2010) 16096-16102.
- [74] S.-J. Ji, S.-N. Ni, F. Yang, J.-W. Shi, G.-L. Dou, X.-Y. Li, X.-S. Wang, D.-Q. Shi, An Efficient synthesis of pyrimido[4,5-b]quinoline and indeno[2',1':5,6]pyrido[2,3-d]pyrimidine derivatives via multicomponent reactions in ionic liquid, *J. Heterocycl. Chem.*, 45 (2008) 693-702.
- [75] S.C. Azimi, Cellulose sulfuric acid catalyzed multicomponent reaction for efficient synthesis of pyrimido and pyrazolo[4,5-b]quinolines under solvent-free conditions, *Iran. J. Catal.*, 4 (2014) 113-120.
- [76] J.M. Khurana, A. Chaudhary, B. Nand, A. Lumb, Aqua mediated indium(III) chloride catalyzed synthesis of fused pyrimidines and pyrazoles, *Tetrahedron Lett.*, 53 (2012) 3018-3022.
- [77] G.K. Verma, K. Raghuvanshi, R. Kumar, M.S. Singh, An efficient one-pot three-component synthesis of functionalized pyrimido[4,5-b]quinolines and indeno fused pyrido[2,3-d]pyrimidines in water, *Tetrahedron Lett.*, 53 (2012) 399-402.
- [78] F. Nemati, R. Saeeedirad, Nano-Fe₃O₄ encapsulated-silica particles bearing sulfonic acid groups as a magnetically separable catalyst for green and efficient synthesis of functionalized pyrimido[4,5-b]quinolines and indeno fused pyrido[2,3-d]pyrimidines in water, *Chin. Chem. Lett.*, 24 (2013) 370-372.
- [79] K. Mohammadi, F. Shirini, A. Yahyazadeh, 1,3-Disulfonic acid imidazolium hydrogen sulfate: a reusable and efficient ionic liquid for the one-pot multi-component synthesis of pyrimido[4,5-b]quinoline derivatives, *RSC Adv.*, 5 (2015) 23586-23590.
- [80] F. Shirini, M.S.N. Langarudi, N. Daneshvar, M. Mashhadinezhad, N. Nabinia, Preparation of a new DABCO-based ionic liquid and investigation on its application in the synthesis of benzimidazoquinazolinone and pyrimido[4,5-b]quinoline derivatives, *J. Mol. Liq.*, 243 (2017) 302-312.